ACS OMEGA

Open Access

http://pubs.acs.org/journal/acsodf

Article

Screening of Multitarget-Directed Natural Compounds as Drug Candidates for Alzheimer's Disease Using *In Silico* Techniques: Their Extraction and *In Vitro* Validation

Sukriti Srivastava, Shilpa Sharma, Shashank Deep, and Sunil Kumar Khare*

Cite This: *ACS Omega* 2023, 8, 38118−38129

Read Online

ACCESS | Metrics & More | Article Recommendations | Supporting Information

ABSTRACT: Alzheimer's disease (AD) is a neurodegenerative disorder that impairs neurocognitive function. Acetylcholinesterase (AChE) and β-site APP cleaving enzyme 1 (BACE1) are the two main proteins implicated in AD. Indeed, the major available commercial drugs (donepezil, rivastigmine, and galantamine) against Alzheimer's are AChE inhibitors. However, none of these drugs are known to reverse or reduce the pathophysiological condition of the disease since there are multiple contributing factors to AD. Therefore, there is a need to develop a multitarget-directed ligand approach for its treatment. In the present study, plant bioactive compounds were screened for their AChE and BACE1 inhibition potential by conducting molecular docking studies. Considering their docking score and pharmacokinetic properties, limonin, peimisine, serratanine B, and withanolide A were selected as the lead compounds. Molecular dynamics simulations of these protein−ligand complexes confirmed the conformational and energetically stabilized enzyme−inhibitor complexes. The inhibition potential of the lead compounds was validated by *in vitro* enzyme assay. Withanolide A inhibited AChE (IC_{50} value of 107 μM) and showed mixed-type inhibition. At this concentration, it inhibited BACE1 activity by 57.10% and was stated as most effective. Both the compounds, as well as their crude extracts, were found to have no cytotoxic effect on the SH-SY5Y cell line.

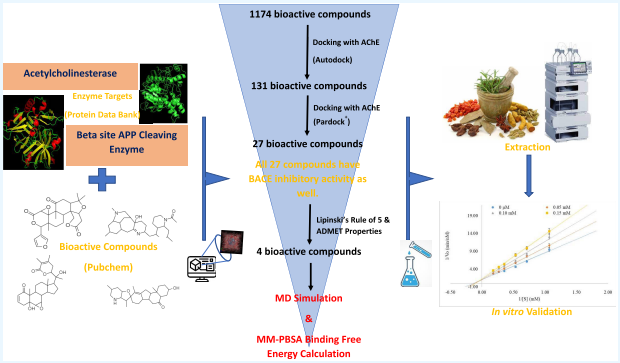

1. INTRODUCTION

Alzheimer's disease (AD) is a progressive cognitive disorder with compromised neurological functions. Prevalent in around 60% of dementia patients, AD has been declared a "global public health priority" by the World Health Organization (WHO) because there is no permanent cure for the disease.[1] The neuropathological condition in the disease is characterized by a reduction in cholinergic neurons, excessive breakdown of the neurotransmitter acetylcholine by acetylcholinesterase (AChE), oxidative stress in neurons, and development of neurofibrillary tangles and Aβ plaques. Various medical approaches targeting these pathological processes have been proven unsuccessful in preclinical or clinical trials, as the cause of the disease is not fully understood.[2] The commercially available anti-Alzheimer's drugs are all AChE inhibitors (donepezil, rivastigmine, and galantamine), except memantine, which targets glutamate excitotoxicity. These drugs target a single aspect that leads to AD and provide only symptomatic relief. Aβ aggregation has been so far the primary therapeutic target for new-age AD therapies. Current research is focused on the reduction in $A\beta_{42}$ production, its aggregation inhibition, disaggregation, and removal from the cerebrospinal fluid. However, all of the potential drugs developed to date have been proved unsuccessful beyond phase II/III clinical trials due to a lack of efficacy. Since multiple factors contribute to the cognitive decline in AD, there is a need to develop a multitarget-directed ligand (MTDL) drug approach to deal with it.[3] The age-old "one target-one molecule" approach cannot alleviate all of the pathologic mechanisms that contribute to AD. Hence, there lies the need to explore molecules that have affinity toward more than one receptor or enzyme, contributing to a particular disease's progression.[4]

Degradation of the neurotransmitter acetylcholinesterase (ACh) by AChE has been identified as one of the major factors of AD. AChE is present in the postsynaptic neurons and neuromuscular regions and is responsible for the transmission of impulses in the central nervous system. Its breakdown by AChE leads to major cognitive failure and degeneration of coordinated muscle movement.[5] Thus, inhibition of AChE reduces the breakdown of ACh in the brain and gives symptomatic relief to the patients. AChE is a carboxylic

Received: June 15, 2023
Accepted: August 18, 2023
Published: October 3, 2023

Table 1. Binding Energies Obtained from Docking of Selected Bioactive Compounds against AChE and BACE Enzyme

S No.	Drug Candidate	Pubchem ID (CID)	AChE		BACE	
			Autodock (kcal/mol)	Pardock (kcal/mol)	Autodock (kcal/mol)	Pardock (kcal/mol)
1	galantamine	5741	−6.5	−8.7	n.a.	n.a.
2	19,20 dihydrotabernamine	44418787	−9.1	−10.13	−9.5	−10.88
3	withanolide M	25090669	−9	−10.47	−9.4	−10.29
4	cannabisin D	71448965	−9	−10.11	−8.6	−10.18
5	α-amyrin	73170	−8.8	−10.18	−8.7	−10.39
6	limonin	179651	−8.6	−10.06	−8.9	−9.94
7	pseudo-obparicine	1.02×10^8	−8.6	−10.85	−10.4	−9.76
8	α-belladonine	21769908	−8.5	−10.15	−8.5	−10.67
9	liquiritic acid	112111	−8.4	−10.08	−8.1	−9.52
10	cannflavin C	25141335	−8.4	−10.06	−9.2	−10.48
11	belladonine	442995	−8.3	−10.65	−9.4	−10.39
12	ursolic acid	64945	−8.2	−11.62	−8.6	−10.26
13	serratanine B	442493	−8.2	−11.15	−9.2	−10.28
14	malibatol A	44575508	−8.2	−9.92	−8.4	−8.55
15	apigenin rutinoside	91740068	−8.2	−9.9	−10	−9.83
16	dauricine	73400	−8.1	−11.98	−9.7	−10.64
17	erythrodiol	101761	−8.1	−10.86	−8.5	−10.12
18	peimisine	161294	−8.1	−9.94	−9.2	−10.17
19	kielcorin	13834128	−8.1	−10.41	−9.2	−10.11
20	B-belladonine	21769909	−8.1	−11.79	−9.7	−9.63
21	haloxysterol C	44407175	−8.1	−10.17	−8.6	−10.51
22	withanolide D	161671	−8	−10.06	−10.4	−10.43
23	morusin 5	5281671	−8	−9.92	−7.8	−9.79
24	4-hydroxylonchocarpin	5889042	−8	−10.23	−9.7	−8.22
25	withanolide A	11294368	−8	−10.09	−9.3	−10.01
26	prenyllicoflavone A	11349817	−8	−9.97	−9.6	−9.37
27	5,7-dihydroxy-6-(2-methylbutanoyl)-8-[(*E*)-3,7-dimethylocta-2,6-dienyl]-4-phenyl-2*H*-chromen-2-one	11351972	−8	−10.89	−9.1	−10.49
28	friedelane	15559345	−8	−9.97	−8.6	−11

https://doi.org/10.1021/acsomega.3c04261
ACS Omega 2023, 8, 38118−38129

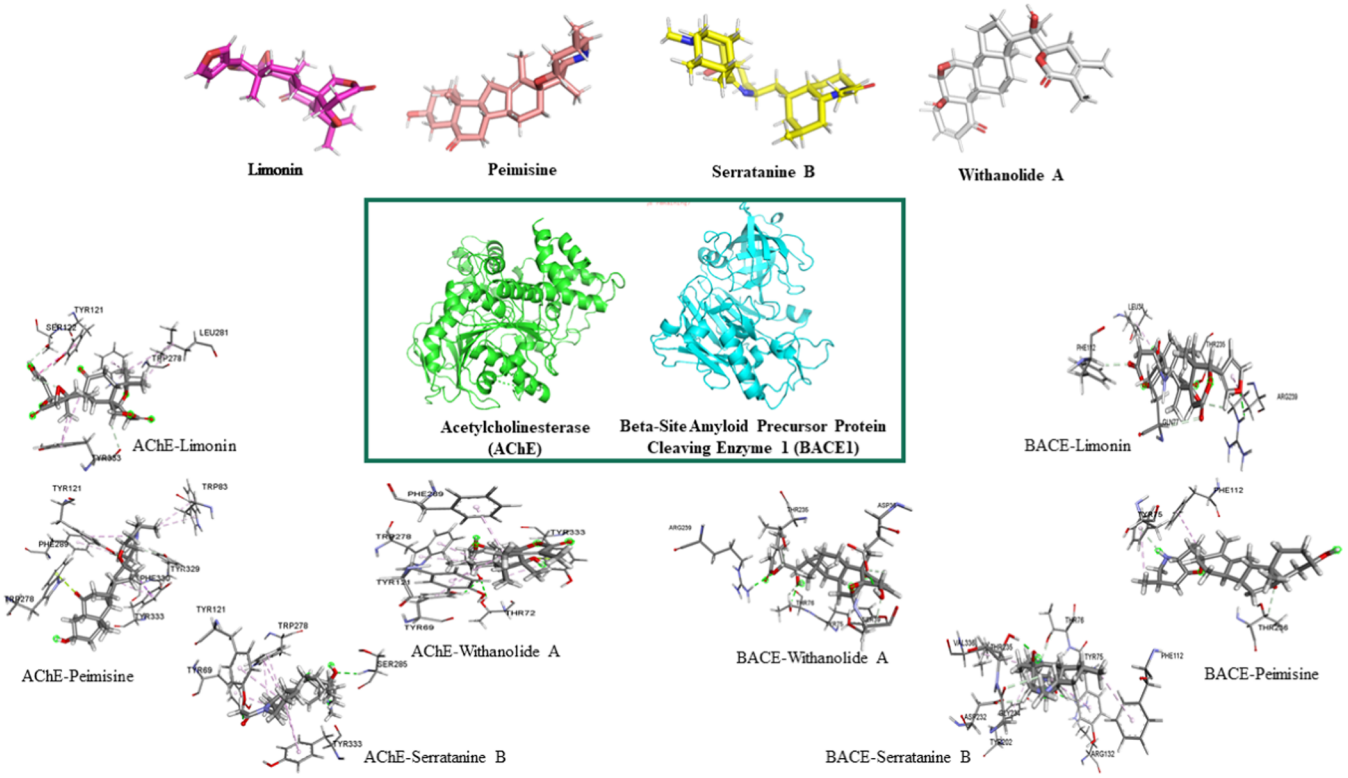

Figure 1. Molecular docking interaction models of AChE and BACE with limonin, serratanine B, peimisine, and withanolide A.

hydrolase of 121.21 kDa containing 2 side chains, with each chain comprising 534 amino acid residues.[6] The catalytic site is marked by the presence of glutamic acid, serine, and histidine in a 20 Å gorge.[7] Direct interaction of any compound with this site causes competitive inhibition of the enzyme, while the compounds interacting with sites other than the catalytic site also inhibit the enzyme by modifying the catalytic site and inducing steric blockade.[8]

Moreover, the transmission of ACh from the presynaptic neuron is also affected by the $A\beta_{42}$ deposition, causing cholinergic dysfunction in the brain, and is identified as an early sign of AD.[9] Usually, the level of ACh decreases in the AD brain. However, ACh accumulates around cholinergic neurons due to the oxidative stress caused by $A\beta_{42}$ plaques and Ca^{2+} signaling excitotoxicity.[10] $A\beta_{42}$ plaque formation is governed by incorrect cleavage of amyloid precursor protein (APP) by β-site APP cleaving enzyme (BACE1) instead of α secretase.[11] Therefore, if BACE1 is inhibited, the formation of insoluble $A\beta_{42}$ will also be reduced.[12] BACE1 is a proteinase/hydrolase of 88.36 kDa containing 2 side chains of 390 amino acid residues each. The catalytic site is marked by the presence of 2 aspartic acid residues, Asp32 and Asp228.[13] Interaction of the bioactive compound with the catalytic site of BACE1 will result in inhibition of its enzyme activity.

India and other south tropical Asian countries are identified as hotspot zones of biodiversity with rich flora. The indigenous traditional knowledge of this flora for various therapeutic applications has also been documented by various researchers.[14] However, the bioactive compounds in plants are usually present along with the other compounds, which might have toxic effects. Thus, there is a need to essentially screen the specific compound responsible for the therapeutic effect of medicinal plants. In this context, the *in silico* screening process for the selection of the target compound before the *in vitro* and *in vivo* screening will save both time and resources.[15] This screening is an important aspect of research, as around 50 and 40% of drug candidates fail because of lower efficacy and high toxicity, respectively.

Considering the above facts, in the present study, screening of bioactive compounds having AChE and BACE1 inhibitory properties was done based on structure-based drug discovery (SBDD). The binding affinity and stability of the interaction between the compounds and the proteins were estimated by employing molecular docking and a subsequent 100 ns molecular dynamic (MD) simulation run.[16] SBDD focuses on the *in silico* protein−ligand interaction. Molecular docking software was used to dock the compounds into the enzyme's active site to obtain their binding energy of interaction. Lower binding energy signifies stronger interaction. This saves time and resources and delivers lead compounds, which are potent enzyme inhibitors. Docking is generally followed by MD simulation. The idea is to simulate a much realistic environment for the protein and ligands to interact for a longer time. The data obtained by running the simulation can give us an actual idea of the changes at the residual level. The stability of the interaction can be foreseen by comparing the variations in the secondary and tertiary structures of the enzyme. Gibb's free energy is the measure of the strength of the interaction. Lower energy indicates stronger ligand binding.

However, the efficiency of a drug molecule does not depend on enzyme inhibition alone. It cannot be administered if it has low absorption or bioavailability and/or higher elimination half-life. It also cannot be administered if it is toxic or forms toxic metabolites. Lipinski's rule of 5 and predicted absorption, distribution, metabolism, elimination, and toxicity (ADMET) properties establish the safety and efficacy of the compound.

https://doi.org/10.1021/acsomega.3c04261
ACS Omega 2023, 8, 38118−38129

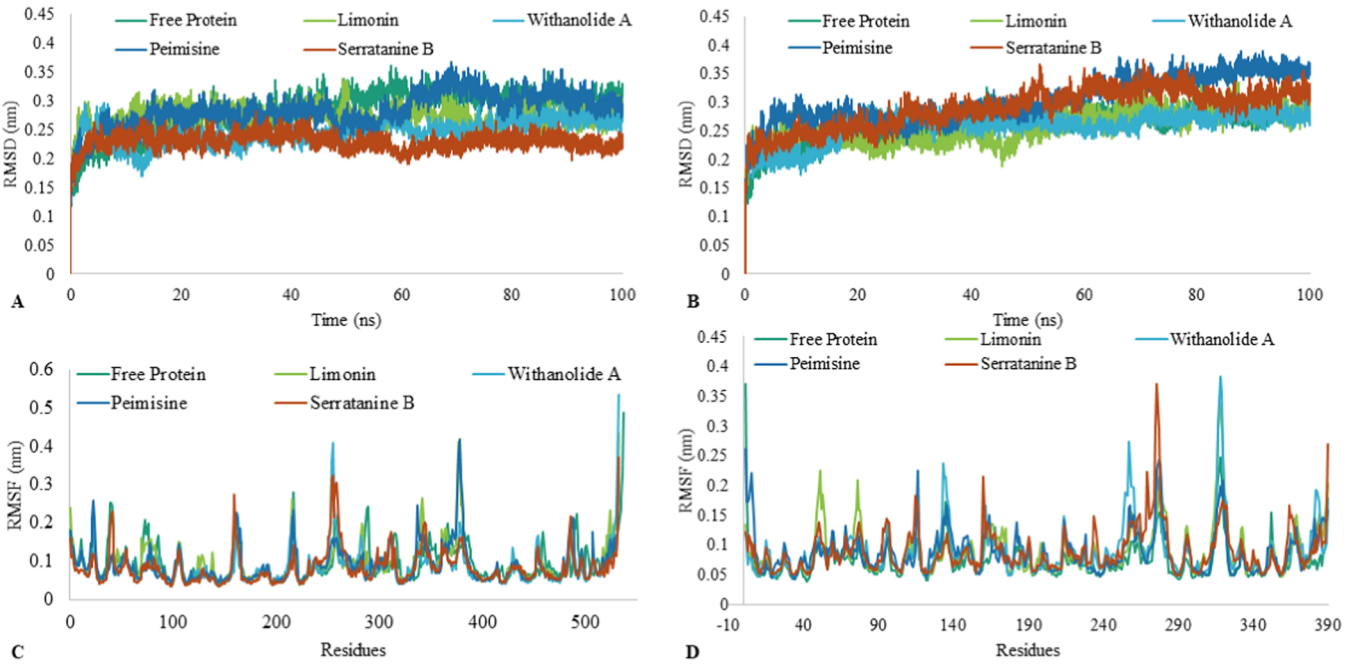

Figure 2. RMSD and RMSF plot of the C_α atoms of AChE and BACE in unbound and bound form. (A) RMSD of AChE and AChE-ligand complex. (B) RMSD of BACE and BACE-ligand complex. (C) RMSF of AChE and AChE-ligand complex. (D) RMSF of BACE and BACE-ligand complex.

Molecular docking and pharmacokinetic profiling together give us compounds that are possibly both effective and safe.[17]

Out of the four compounds obtained from computational analysis, we chose withanolide A and limonin for extraction and *in vitro* studies,[18] as the other compounds were unavailable. In the past, few *in silico* studies have shown withanolide A to be a potent inhibitor of AChE[19−21] and BACE1 activity,[22] supporting our findings. The *in silico* data need to be validated *in vitro* before any *in vivo* studies. *In vitro* analysis offers a better understanding of the mechanistic effect of the drug candidate on the enzyme. It provides numerical data on how efficient a drug is by determining the IC_{50} value of the drug, and enzyme kinetic parameters define the type of inhibition.

2. RESULTS AND DISCUSSION

2.1. Selection of 4 Natural Inhibitors of AChE and BACE1 Activity, Based on Their Affinity and Pharmacokinetic Properties Obtained from Computational Analysis. To screen AChE inhibitors, binding energy scores were calculated from docking analysis of the interaction of AChE with the listed bioactive compounds and galantamine. The binding energy of the AChE-galantamine interaction was −6.5 kcal/mol. The binding energy of 883 compounds was lower than −6.5 kcal/mol. Among them, only 131 compounds had a binding energy lower than −8 kcal/mol as determined by AutoDock (Table S1). On secondary screening of the selected AChE inhibitors using ParDOCK, only 27 compounds having a binding energy of interaction lower than −10 kcal/mol were finally shortlisted for further screening. The docking of these molecules was also carried out with BACE1. BACE1 interacts with potential AChE inhibitors with binding energies lower than −8 kcal/mol. The binding energies obtained from docking of selected bioactive compounds against AChE and the BACE1 enzyme are reported in Table 1.

The safety and efficacy of a drug molecule are of primary concern. *In silico* pharmacokinetic profiling of the molecule has proven to be useful in the effective discovery of a drug. Thus, Molinspiration Cheminformatics was used in this study to determine the drug-likeness of small molecules (Table S2). Table S3 shows the ADMET-associated drug-like parameters of the hit compounds. Among all of the compounds, only limonin, peimisine, serratanine B, and withanolide A were shortlisted based on *in silico* pharmacokinetic profiling. Figure 1 shows the interaction of AChE and BACE1 with the lead compounds, while Figure S1 depicts the two-dimensional (2D) structure of the lead compounds. Table S4 depicts the amino acid residues interacting with the respective ligands with bond lengths ≤5 Å during docking studies.

2.2. Interaction and Binding Analysis between AChE/BACE1 and the Lead Compounds through MD Simulation. MD simulation of the lead compounds selected based on docking and pharmacokinetic profiling was done. The interaction of the target enzymes with the lead compounds was observed for 100 ns. All of the simulations were repeated 3 times, and the average values were plotted to determine the stability of the enzyme-ligand interaction.

To determine the stability of the protein−ligand interaction, the root-mean-square deviation (RMSD) and root-mean-square fluctuation (RMSF) of the Cα atoms of the protein at different time points were monitored (Figure 2A,B). The difference in RMSD values of the bound and unbound AChE as well as BACE1 remained lower than 0.1 nm in the case of all of the AChE-ligand complexes. A lower RMSD value signifies stable interaction between the enzyme and the bioactive compound. RMSF graphs of both AChE and the BACE1 protein−ligand complex were assessed to determine the effect of ligand binding on the amino acid residues during the last 25 ns of interaction. As depicted in Figure 2C,D, the amino acid residues showing any fluctuation with respect to the Cα atoms of the free protein were present in the random coil region and

https://doi.org/10.1021/acsomega.3c04261
ACS Omega 2023, 8, 38118−38129

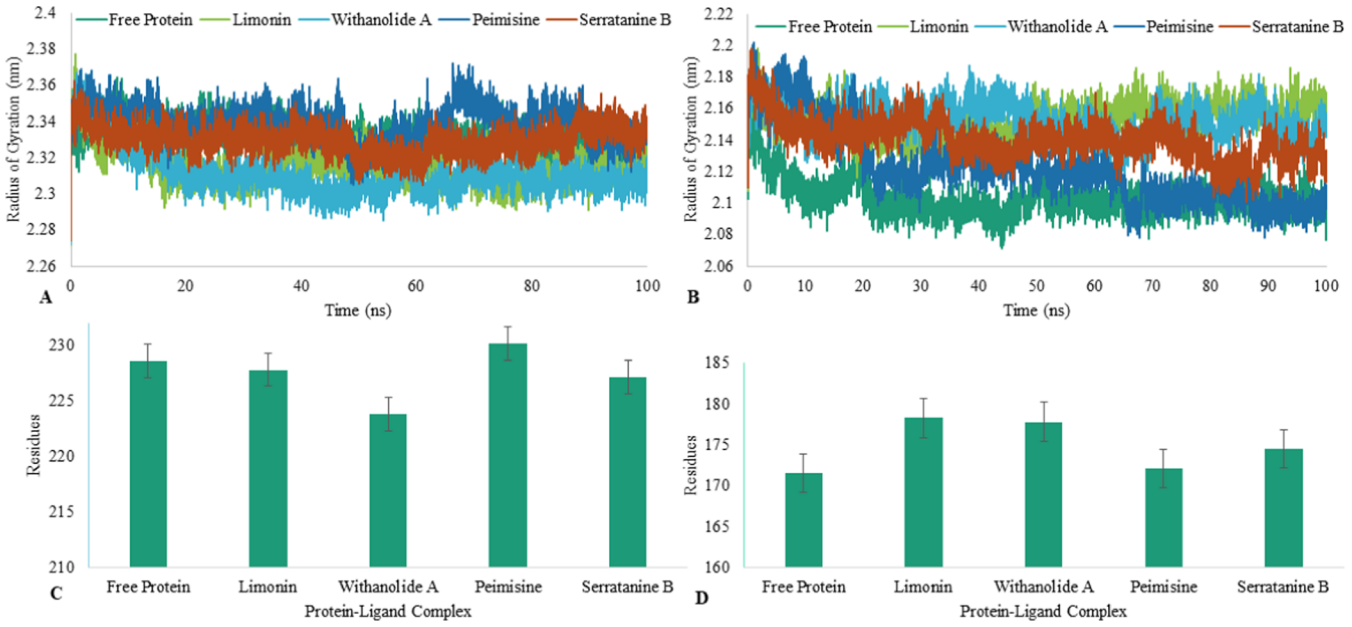

Figure 3. Radius of gyration (R_g) and solvent-accessible surface area (SASA) of AChE and BACE in unbound and bound form. (A) R_g of AChE and AChE-ligand complex. (B) R_g of BACE and BACE-ligand complex. (C) SASA of AChE and AChE-ligand complex. (D) SASA of BACE and BACE-ligand complex.

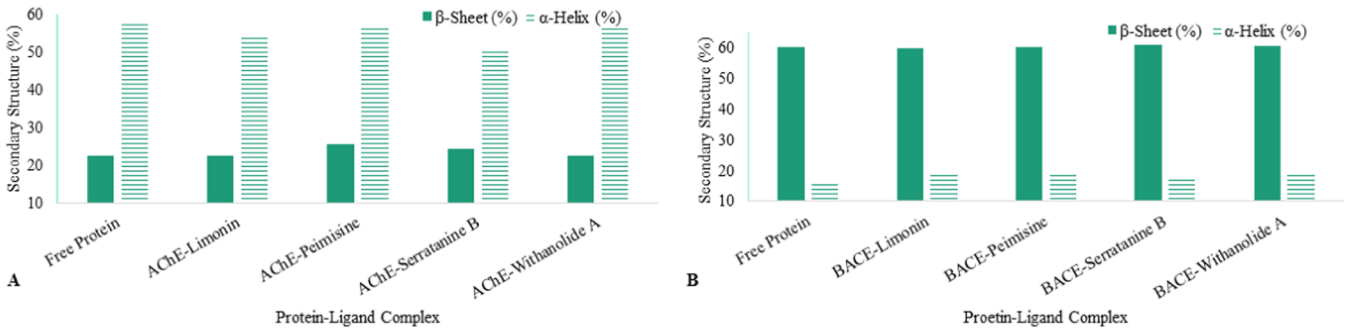

Figure 4. Secondary structure change in AChE (A) and BACE (B) while interacting with the bioactive compounds.

would possibly not affect the protein−ligand binding. In all of the protein−ligand complexes, amino acids PHE287, ARG288, and PHE289 lying in the coil region of the ligand-binding site of AChE showed fluctuation while interacting with the lead compounds. Similarly, in the case of BACE1, only ILE390 showed fluctuation among all of the protein−ligand complexes. The amino acid residues in the complexes did not show any prominent fluctuation during the interaction.

The radii of gyration (R_g) and solvent-accessible surface area (SASA) of AChE and BACE1 in both unbound and bound forms were compared, and the results are shown in Figure 3A−D. While interacting with the AChE protein, the R_g value of AChE increased in the presence of peimisine, whereas it decreased in the presence of withanolide A and remained almost unchanged in the presence of serratanine. In the case of BACE1, the R_g value of the protein increased in the presence of all of the three proteins. However, the increase in R_g was less than 0.1 nm. The results from SASA analysis further corroborate with the data obtained from R_g analysis. Withanolide A on binding with AChE reduced the SASA and peimisine increased it, while limonin and serratanine B had no visible effect on it. No effect on SASA was observed after the binding of compounds to BACE1. There was no significant difference in the R_g and SASA values of all of the protein−ligand complexes in comparison to the free AChE and BACE1. The results showed that during the 100 ns simulation, the enzyme did not lose its three-dimensional (3D) structure.

The change in secondary structure content (SSC) of the target enzyme was measured in terms of the α-helix and β-sheet contents of the protein in the presence of the bioactive compound, as shown in Figure 4. There was the least change in α-helix and β-sheet content in the case of AChE-withanolide A interaction, followed by AChE-limonin interaction. In the case of the BACE1 enzyme, α-helix, and β-sheet content remained the same post the enzyme−inhibitor interaction. This was further confirmed by the database of secondary structure assignments (DSSP) plot of the secondary structure data of the proteins, as seen in Figure S2. Based on the structural stability of the enzyme in the presence of the natural inhibitors, withanolide A and limonin are expected to be the most potent natural inhibitors of AChE and BACE1 enzymes.

We performed the molecular mechanics Poisson−Boltzmann surface area (MM-PBSA) analysis for the determination of the binding energy of protein−ligand interaction. The last 10 ns of the 100 ns trajectory obtained from the MD simulation was used for the calculation. The low binding energy of all of the protein−ligand complexes affirmed the strong interaction between them, as depicted in Table 2.

https://doi.org/10.1021/acsomega.3c04261
ACS Omega 2023, 8, 38118−38129

Table 2. Binding Free Energy, of the Enzyme-Inhibitor Complex, Obtained by the MM-PBSA Approach (n = 3)

complex	$\Delta E_{\text{vander Waal}}$ (kJ/mol)	$\Delta E_{\text{electrostatic}}$ (kJ/mol)	$\Delta E_{\text{polar solvation}}$ (kJ/mol)	$\Delta E_{\text{non-polar}}$ (kJ/mol)	$\Delta E_{\text{binding}}$ (kJ/mol)
AChE-limonin	−177.78 ± 8.89	−26.55 ± 1.33	90.28 ± 4.51	−18.25 ± 0.91	−132.31 ± 6.62
AChE-peimisine	−220.41 ± 11.02	−8.38 ± 0.42	70.40 ± 3.52	−23.82 ± 1.19	−182.21 ± 9.11
AChE-serratanine B	−230.22 ± 11.51	−13.14 ± 0.66	85.53 ± 4.28	−26.23 ± 1.31	−184.06 ± 9.20
AChE-withanolide A	−189.00 ± 9.45	−22.00 ± 1.10	89.02 ± 4.45	−20.47 ± 1.02	−142.45 ± 7.12
BACE-limonin	−189.84 ± 9.49	−24.06 ± 1.20	92.14 ± 4.61	−19.36 ± 0.97	−141.12 ± 7.06
BACE-peimisine	−192.76 ± 9.64	−24.26 ± 1.21	163.64 ± 8.18	−21.04 ± 1.05	−74.43 ± 3.72
BACE-serratanine B	−160.74 ± 8.04	−22.14 ± 1.11	99.76 ± 4.99	−20.41 ± 1.02	−103.53 ± 5.18
BACE-withanolide A	−177.44 ± 8.87	−40.23 ± 2.01	144.59 ± 7.23	−20.28 ± 1.01	−93.36 ± 4.67

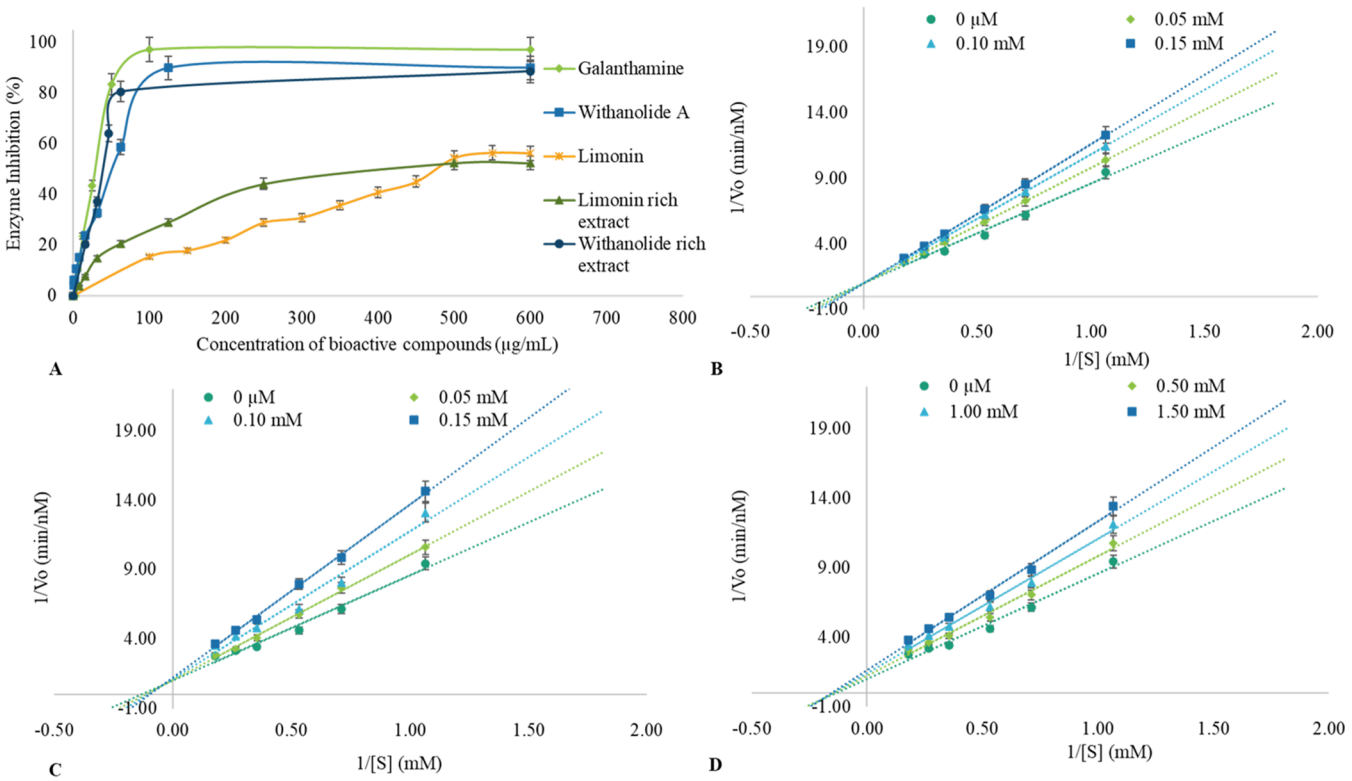

Figure 5. IC_{50} determination (A) and Lineweaver−Burk plot for AChE enzyme inhibition by (B) galantamine, (C) withanolide A, and (D) limonin (n = 3; $p < 0.01$, two-tailed t-test).

Peimisine (−182.21 ± 9.11 kJ/mol) and serratanine B (−184.06 ± 9.20 kJ/mol) were observed to have lower binding energies than limonin (−132.31 ± 6.62 kJ/mol) and withanolide A (−142.45 ± 7.12 kJ/mol) with the AChE enzyme. For the BACE1 enzyme, limonin had the lowest binding energy (−141.12 ± 7.06 kJ/mol), followed by serratanine B (−103.53 ± 5.18 kJ/mol), withanolide A (−93.36 ± 4.67 kJ/mol), and peimisine (−74.43 ± 3.72 kJ/mol).

2.3. Extraction of Limonin and Withanolide A from Their Plant Source. As described, withanolide A and limonin were extracted by an ultrasound-assisted solvent polarity gradient approach from *Withania somnifera* and *Citrus limon*, respectively. Withanolide A was obtained in the butanol fraction. The concentration of withanolide A in the extract was 134.97 µg/mg of the extract as quantified by high-performance liquid chromatography (HPLC). The absorbance peak was observed using a UV-diode array detector at wavelength 228 nm. The peak for standard withanolide A appeared at 27 min. Limonin was present in the ethyl acetate fraction. The concentration of limonin in the extract as estimated by high-performance liquid chromatography (HPLC) was 245.21 µg/mg of the extract. The absorbance peak was observed using a UV-diode array detector at wavelength 210 nm. The peak for standard limonin appeared at 4.78 min.

2.4. Validation of the AChE and BACE Inhibition Activity of the Selected Compounds. The AChE inhibition potential of the lead compounds was determined in terms of their half-maximal inhibitory concentration (IC_{50}) value from the linear regression of the enzyme activity graph, Figure 5(A). Data were plotted as the mean of three biological repeats and were conducted in triplicates. The IC_{50} value of galantamine, withanolide A, and limonin was determined to be 0.104 ± 0.01, 0.107 ± 0.01, and 1.057 ± 0.05 mM, respectively. The withanolide-rich extract and limonin-rich extract were also analyzed for their enzyme inhibition potential, and their IC_{50} values for AChE inhibition were 0.0368 and 0.488 mg/mL of the extract, respectively. At 0.1 mM concentration, limonin showed the highest inhibition of BACE1 activity (60.7 ± 3.04%), followed by withanolide A (57.1 ± 2.86%), limonin-rich extract (53.0 ± 2.65%), and

https://doi.org/10.1021/acsomega.3c04261
ACS Omega 2023, 8, 38118−38129

withanolide-rich extract (51.9 ± 2.60%). Quercetin showed the least inhibition (41.3 ± 2.07%), Figure S3.

The Lineweaver−Burk plot was used to determine the enzyme inhibition kinetics of AChE activity in the presence of the bioactive compounds (Figure 5B−D). The IC_{50}, K_m, and V_{max} values of the enzyme are shown in Table 3. Galantamine inhibited AChE by a competitive inhibition model; i.e., it competes with the natural substrate of the enzyme and inhibits it by binding at the catalytic site. Withanolide A followed a mixed inhibition model. V_{max} decreased and K_m increased with the increase in concentration of the compound, implying that withanolide A binds at both the catalytic as well as the allosteric site of the enzyme. Limonin followed the uncompetitive inhibition model, and both V_{max} and K_m decreased with the increase in its concentration, implying that the compound binds to the allosteric site of the enzyme−substrate complex only.

2.5. Cytotoxic Effect of the Compounds on the SH-SY5Y Cell Line. MTT assay was performed on the SH-SY5Y cell line to study the cytotoxic effect of the bioactive compounds. Withanolide A, withanolide-rich extract, and limonin showed 100% cell viability until 100, 50, and 10 μg/mL concentration, respectively (Figure 6). Even at a high concentration of 200 μg/mL, the compounds showed insignificant cytotoxicity.

3. CONCLUSIONS

In the present study, plant bioactive compounds were screened computationally to obtain AChE and BACE1 inhibitors. Some compounds were selected based on the docking score obtained from the molecular docking studies. By subjecting the selected compounds to the pharmacokinetic assessment, established for the oral drugs, based on their ADMET properties and Lipinski's rule of 5, we obtained four lead compounds, including limonin, peimisine, serratanine B, and withanolide A. The MD simulation run of 100 ns suggested a stable interaction between these compounds and both the enzymes, AChE and BACE1, respectively. The interaction of AChE with withanolide A and limonin reduced the radius of gyration and the solvent-accessible surface area, which implies that the interaction makes the enzyme structure more compact. The compact structure of the enzyme limits the accessibility of the enzyme's active site to its natural substrate, further inhibiting the enzyme's activity. The estimated binding free energy of withanolide A's interaction with AChE was −142.45 kJ/mol, and that of BACE1 was −93.36 kJ/mol.

The *in silico* findings of enzyme inhibition were validated by the *in vitro* enzyme inhibition activity of pure withanolide A and limonin as well as their extracted form. Galantamine (104 μM) and withanolide A (107 μM) showed similar IC_{50} values against AChE, much higher than that of limonin (1.057 mM). The enzyme kinetic studies demonstrated that galantamine is a competitive inhibitor, withanolide A follows mixed-type inhibition, and limonin follows uncompetitive type inhibition. BACE1 inhibition in the presence of 10 μg/mL withanolide A (57.10%) was slightly lower than that of limonin (60.69%). However, both compounds exhibited better inhibition than the reference compound, quercetin (41.26%). The compounds were found to have no cytotoxic effect on the SH-SY5Y cell line, as determined by conducting MTT assay. From the *in silico* and *in vitro* studies, it can be deduced that withanolide A is a potential AChE and BACE1 inhibitor and can be a potential drug molecule against Alzheimer's disease. Nonethe-

Table 3. Kinetic Parameters of the AChE Enzyme in the Presence of Bioactive Inhibitors ($n = 3$; $p < 0.01$, Two-Tailed *t*-Test)

		galantamine (reference)				withanolide A			limonin	
Kinetic Parameter	control	0.05 mM	0.10 mM	0.15 mM	0.05 mM	0.10 mM	0.15 mM	0.5 mM	1.00 mM	1.50 mM
IC_{50} value (mM)	n.a.	0.104 ± 0.01			0.107 ± 0.01			1.057 ± 0.05		
V_{max} (ΔA/min)	1.00 ± 0.05	1.00 ± 0.05	1.00 ± 0.05	1.00 ± 0.05	0.97 ± 0.05	0.87 ± 0.04	0.81 ± 0.04	0.83 ± 0.04	0.71 ± 0.03	0.62 ± 0.03
K_m (mM)	7.57 ± 0.38	8.76 ± 0.44	9.76 ± 0.49	10.55 ± 0.53	8.73 ± 0.44	9.25 ± 0.46	10.07 ± 0.50	7.13 ± 0.36	6.82 ± 0.34	6.59 ± 0.33

https://doi.org/10.1021/acsomega.3c04261
ACS Omega 2023, 8, 38118−38129

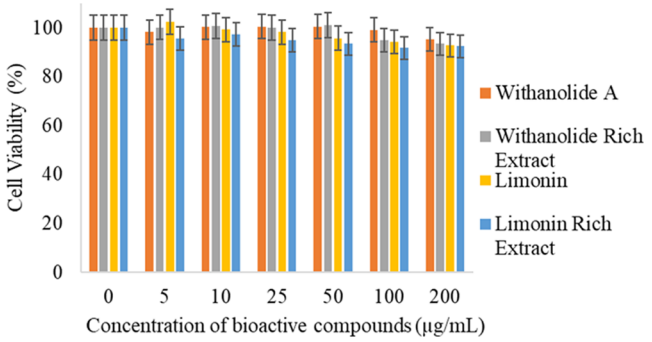

Figure 6. Effect of the selected bioactive compounds on the cell viability of the SH-SY5Y cells ($n = 3$; $p < 0.01$, two-tailed t-test).

less, *in vivo* studies need to be performed to confirm the effectiveness and efficacy of the compound. Additionally, incorporating these bioactive compounds into our routine diet can improve neurological health and prevent or delay the process of neurodegeneration.

4. METHODS

4.1. Instrumentation and Materials. The C-18 column HPLC (Agilent Technologies, 12,000 Infinity) was used to quantify the compound in plant extracts, absorbance values were recorded by a microplate spectrophotometer reader (ThermoFisher Scientific, India), and relative fluorescence was determined by a fluorescence spectrometer (PerkinElmer LS55, U.K.). Chemicals such as AChE (from *Electrophorus electricus*), acetylthiocholine, recombinant BACE1 (from HEK 293 cells), BACE1 fluorogenic substrate IV, DTNB dye, galantamine, commercial limonin, quercetin, and withanolide A were purchased from Sigma-Aldrich, India. Lemon seeds and Ashwagandha roots were procured from a local market. The SH-SY5Y cell line was purchased from the National Centre for Cell Science (NCCS), Pune. The antibiotic antimycotic solution (10,000 U penicillin, 10 mg streptomycin, and 25 μg Amphotericin B), Dulbecco's phosphate-buffered saline (DPBS), fetal bovine serum (FBS), nutrient mixture F-12 Ham, and trypsin-EDTA solution 1× required for mammalian cell culture were procured from HiMedia, India. 3-(4,5-Dimethylthiazol-2-yl)-2,5-diphenyltetrazolium bromide (MTT) was obtained from Merck, Germany. All of the chemicals used were of analytical grade.

4.2. Phytochemical Retrieval and Preparation. A library of bioactive compounds having neuroprotective properties was prepared based on the literature and traditional knowledge.[24,25] The 3D structures of these compounds were retrieved from PubChem (https://pubchem.ncbi.nlm.nih.gov//) in the structure data file (.sdf) format.[26] These structures were converted to .pdb files using OpenBabel (https://sourceforge.net/projects/openbabel/). The 3D crystal structure of the enzymes, viz. AChE (PDBID 4M0E)[27] and BACE1 (PDBID 3CIB),[28] were retrieved from Protein Data Bank in .pdb file format. Minor modifications in the enzyme structure were done using PyMOL software (PyMOL Molecular Graphics System, Version 1.2r3pre, Schrödinger, LLC).[29] All of the additional side chains, heteroatoms, and water molecules were removed, and hydrogen atoms were added to the structure. Galantamine was used as the reference drug during all of the computational studies.

4.3. Docking Analysis. AutoDock4 was used for the primary screening of the bioactive compounds based on their binding affinity against AChE.[30] The selected compounds were rescreened using ParDOCK.[31] Both AutoDock4 and ParDOCK were used to screen the compounds for their binding affinity against BACE1. After the protein was loaded on AutoDock, the missing residues were repaired. Kollman and Gasteiger charges were added to the protein and the ligand molecules, respectively. Once the protein was prepared, a ligand was added, and the number of active torsions of the ligand was kept below 32. To be able to work with receptors and ligands on AutoDock, they were converted to receptor.pdbqt and ligand.pdbqt file, respectively. Docking was performed to obtain the binding energy of the enzyme-compound complex. The complex with the lowest binding energy was chosen for further analysis. The interaction between the protein−ligand complex was observed using the Discovery Studio visualizer.[32]

4.4. Pharmacokinetic Properties of the Selected Bioactive Compounds. To test the permeation/absorption of the bioactive compounds by the cells, when administered orally, the pharmacokinetic characteristics of the compounds were determined, as per Lipinski's rule of 5, using the online tool Molinspiration (https://www.molinspiration.com). Each of the selected bioactive compounds was analyzed for its molecular weight ($M_W < 500$ Da), number of hydrogen bond acceptors (nOH $\leq$ 10), number of hydrogen bond donors (nOHNH $\leq$ 5), and partition coefficient ($\log P$ value $\leq$ 5) according to the rule.[33]

The ADMET properties, viz. absorption, distribution, metabolism, elimination, and toxicology of a compound inside the body, were also estimated using admetSAR.[34] The compounds following Lipinski's rule with acceptable ADMET properties were selected for further studies.

4.5. Molecular Dynamic Simulation. The input for MD simulation was the enzyme-compound complex obtained after docking studies. Simulations were carried out using the GROMOS96 54a7 force field on Groningen machine for chemical software (GROMACS),[35,36] which results in the generation of a protein topology file and a .gro processed protein structure file for GROMACS. Automated Topology Builder and Repository 3.0 (ATB) was used to write the topology of the ligand.[37] A combined topology file was prepared for both protein and ligand; afterward, an aqueous system was created for the protein−ligand complex by solvating it with water molecules, and the protein was neutralized by adding charges. Moreover, to avoid any inappropriate geometry of the protein or steric clashes, the energy of the system was minimized. To stabilize the MD trajectories, the temperature and pressure of the system were equilibrated and optimized for 100 ps under an NVT and NPT ensemble. After completely optimizing the system, the production MD run was executed thrice for 100 ns to obtain the trajectories at different time points.[38]

4.6. Analysis of MD Trajectory. To confirm the stability of the protein−ligand interaction, the RMSD of the complex from the reference structure (first frame) was monitored. For all of the analyses, C_α atoms of the protein were taken into consideration. For studying the individual residual fluctuation in a complex, RMSF values for the last 25 ns of the simulation were observed. The regions and residues involved in the high-fluctuation region were particularly noted.[39] The Rg and SASA of the protein in the complex were determined to state the effect of the interaction on the folding and unfolding of the protein. Changes in protein secondary structure were also

https://doi.org/10.1021/acsomega.3c04261
ACS Omega 2023, 8, 38118−38129

calculated and DSSP graphs were plotted to record the structural differences in protein before and after interaction with ligand.[33,40]

4.7. MM-PBSA Analysis. To determine Gibb's free energy of protein−ligand interaction, the molecular mechanics Poisson−Boltzmann surface area (G_MMPBSA) approach was used.[41] The binding energy of the complex was estimated for all of the lead compounds with AChE and BACE1. The trajectories obtained after running 100 ns of MD simulation were utilized for the calculations.

$$\Delta G_{\text{binding}} = \Delta G_{\text{complex}} - (\Delta G_{\text{protein}} + \Delta G_{\text{ligand}}) \quad (1)$$

$$\Delta G_{\text{binding energy}} = \Delta E_{\text{MM}} - TS + \Delta G_{\text{solvation}} \quad (2)$$

$$\Delta E_{\text{MM}} = \Delta E_{\text{bonded}} + \Delta E_{\text{non-bonded}} \quad (3)$$

$$\Delta G_{\text{solvation energy}} = \Delta G_{\text{polar solvation energy}} + \Delta G_{\text{non-polar solvation energy}} \quad (4)$$

TS in eq 2 denotes the entropic contribution to the free energy in a vacuum where T and S represent the temperature and entropy, respectively. For comparison of the binding energies of various ligands to the same receptor, entropy contributions were not considered. In eq 3, the bonded interaction energy (ΔE_{bonded}) was considered to be zero while determining the molecular mechanics energy (ΔE_{MM}) since, in a single-trajectory approach, the conformation of both bound and unbound protein and ligand is assumed to be the same. The nonbonded interaction energy ($\Delta E_{\text{non-bonded}}$), majorly Van der Waal and electrostatic interaction, between the protein and ligand account for ΔE_{MM}. For the final calculation of the binding free energy of interaction, eq 5 was used.[42]

$$\Delta G_{\text{binding energy}} = \Delta G_{\text{van der Waals}} + \Delta G_{\text{electrostatic}} + \Delta G_{\text{polar solvation}} + \Delta G_{\text{non-polar solvation}} \quad (5)$$

4.8. Extraction of Bioactive Compounds from Their Plant Source. Due to the unavailability of peimisine and serratanine B compounds in pure form as well as their plant sources in India, we could not validate their potential *in vitro*. However, withanolide A and limonin with the next high $\Delta G_{\text{binding energy}}$ were extracted from *Withania somnifera* (Ashwagandha) and *Citrus limon* (Lemon), respectively,[43] using the ultrasound-assisted sequential polarity gradient extraction technique.[44]

Withanolides are localized in the roots of the Ashwagandha plant and limonin in the lemon seeds. The respective plant parts were obtained from a local market. The plant parts were surface sterilized with 70% ethanol, followed by a 5% sodium hypochlorite solution. Afterward, the parts were washed with distilled water and finally sun-dried. The dried plant material was macerated to a powder in a mortar pestle. The powdered root extract was washed with 80% methanol. The mixture was filtered to obtain the filtrate, which was dried on a rotary evaporator to get a crude extract. The extract was further washed with hexane, followed by the addition of dichloromethane, ethyl acetate, and butanol. The butanol fraction was dried on the rotary evaporator to obtain a withanolide-rich extract.[45] For the detection and quantification of withanolide A present in the extract, the solvent fraction was run through the C-18 HPLC column (Agilent Technologies, 12000 Infinity) at column temperature 37 °C. The mobile phase used methanol and 0.01 M ammonium acetate buffer (pH 5.0), in the ratio 60:40, and the flow rate was kept constant at 1.0 mL/min.[23] The limonin-rich fraction was extracted from the lemon seeds. The powdered seed extract was first defatted with hexane and then washed with ethyl acetate.[26] The ethyl acetate fraction was dried to obtain a limonin-rich extract. For detection and quantification of limonin in the extract, it was run through a C-18 HPLC column at 37 °C. Water and acetonitrile, in the ratio 30:70, were used as the mobile phase, and the flow rate was kept constant at 0.5 mL/min.

4.9. *In Vitro* AChE Inhibition. AChE inhibition by the lead bioactive compounds was confirmed by conducting the Ellman assay.[46] The enzyme stock solution was prepared in 0.1 M Tris−HCl (pH 7.5) and stored at −20 °C. The enzyme assay was done in a 96-well plate, with a final reaction volume of 100 μL. The assay mixture contained 30 μL of the test compound, dissolved in 10% (v/v) methanol, 10 μL of 0.5 U AChE enzyme, prepared in Tris-HCl (pH 7.4), and 50 μL of 5,5′-dithiol-bis(2-nitrobenzoic acid) (DTNB) dye. The mix was incubated at 37 °C for 15 min for binding with the enzyme. Thereafter, the substrate acetylthiocholine iodide was added to the well, and the increase in absorbance was monitored at 412 nm.[47] Galantamine was used as a reference. Based on enzyme activity, the inhibitory potential of the commercial and extracted compounds was determined, and the IC_{50} value was calculated. The inhibition potential of the extracted compounds was compared with commercially available withanolide A and limonin.

$$\text{enzyme inhibition (\%)} = \frac{E_o - E_s}{E_o} \times 100 \quad (6)$$

Enzyme inhibition was calculated by employing eq 6, where E_o is the enzyme activity in the presence of substrate alone, while E_s is the enzyme activity in the presence of substrate, as well as the plant compound. Enzyme activity was measured in terms of absorbance. IC_{50} value was determined graphically by linear regression analysis of the enzyme activity and the concentration of the compound.

4.10. Enzyme Kinetic Study. For this, the nature of enzyme inhibition was characterized based on its kinetic properties, estimated through Lineweaver−Burk plot analysis. AChE inhibition was studied at different concentrations of the substrate, acetylthiocholine, in the presence of a varying concentration of pure compounds.[46]

4.11. *In Vitro* BACE1 Inhibition. The BACE1 inhibition potential of withanolide A, limonin, and their plant extracts was estimated by using recombinant BACE1, expressed in HEK 293 cells, assayed against a sequence-specific BACE1 substrate (FRET peptide, EDANS-EVNLDAEF-DABCYL). The enzyme stock solution was prepared in 0.1 M Tris−HCl (pH 7.5), and substrate stock solution was prepared in 50 mM ammonium bicarbonate and stored at −20 °C. The reaction mixture was prepared in 50 mM sodium acetate assay buffer, pH 4.5, containing BACE1 (1.0 U/mL), substrate (750 nM), and the test compounds (10.0 μg/mL),[48] Quercetin was used as the reference drug. After incubation for 60 min at 25 °C in the dark, 2.5 M sodium acetate was added to stop the reaction. The relative fluorescence intensity was observed at an excitation wavelength of 530 nm and an emission wavelength of 545 nm on a fluorescence spectrometer.[49]

https://doi.org/10.1021/acsomega.3c04261
ACS Omega 2023, 8, 38118−38129

4.12. MTT Assay. The neuroblastoma cell line, SH-SY5Y, was maintained in a nutrient mixture (F-12 Ham) supplemented with 10% FBS and 1% antibiotics. The cells were incubated at 37 °C in a humidified environment with 5% CO_2.[50]

The cytotoxicity of all four samples, including withanolide A, withanolide-rich extract, limonin, and limonin-rich extract, was studied by conducting MTT assay. The SH-SY5Y cells were seeded in a 96-well plate, with a density of 5×10^3 cells/well. After 24 h of incubation, cells were treated with fresh growth media containing different concentrations of samples (0−200 μg/mL). The cells were incubated again for 24 h. Thereafter, the cells were washed with DPBS and incubated with 0.5 mg/mL of MTT solution for 4 h at 37 °C and 5% CO_2. After incubation, the MTT solution was removed, and the formazan crystals formed were dissolved in 100 μL of DMSO.[51] After 20 min of incubation, the absorbance of the product was measured at 595 nm using a microplate reader (Multiskan Sky Microplate Absorbance Reader, Thermo Scientific, Singapore). Cells containing only growth media without samples were taken as control.

4.13. Statistical Analysis. All of the values were depicted as mean ± SEM. Group differences were analyzed using two-tailed t test, setting the statistical significance at $p < 0.01$.

■ ASSOCIATED CONTENT

Supporting Information

The Supporting Information is available free of charge at https://pubs.acs.org/doi/10.1021/acsomega.3c04261.

Additional computational and experimental results; binding energy obtained from docking studies of phytochemicals with AChE using Autodock 4; Lipinski's rule of 5 applied to the hit compounds to determine their drug-likeness; ADMET properties stating absorption, distribution, metabolism, and toxicity associated drug-like factors of the hit compounds; amino acid residues interacting with the respective ligands for both AChE and BACE; 2D structure of the lead compounds selected for performing MD simulation; DSSP plot of secondary structure change of AChE and BACE; BACE inhibition in the presence of quercetin, withanolide A, withanolide-rich extract, limonin, and limonin-rich extract (PDF)

■ AUTHOR INFORMATION

Corresponding Author

Sunil Kumar Khare − *Enzyme and Microbial Biochemistry Laboratory, Department of Chemistry, Indian Institute of Technology Delhi, New Delhi 110016, India;* orcid.org/0000-0002-7339-3058; Phone: +911126596533; Email: skkhare@chemistry.iitd.ac.in, skhare@rocketmail.com; Fax: +911126581102

Authors

Sukriti Srivastava − *Enzyme and Microbial Biochemistry Laboratory, Department of Chemistry, Indian Institute of Technology Delhi, New Delhi 110016, India*

Shilpa Sharma − *Biophysical Chemistry Laboratory, Department of Chemistry, Indian Institute of Technology Delhi, New Delhi 110016, India*

Shashank Deep − *Biophysical Chemistry Laboratory, Department of Chemistry, Indian Institute of Technology Delhi, New Delhi 110016, India;* orcid.org/0000-0002-4908-8205

Complete contact information is available at: https://pubs.acs.org/10.1021/acsomega.3c04261

Author Contributions

conceptualization, supervision, review, and editing, S.D.; *in silico* work, experimentation, formal analysis, and writing of the original draft, S.S.; methodology and review, S.S.; review and editing, S.K.K. All authors have read and agreed to the published version of the manuscript.

Notes

The authors declare no competing financial interest.

■ ACKNOWLEDGMENTS

The authors are thankful to the institute for providing the fellowship. The authors thank the IIT Delhi high power computing (HPC) and supercomputing facility (SCF-Bio) for providing the computational resources. The authors are grateful to Prof. Prashant Mishra, Department of Biochemical Engineering & Biotechnology, IIT Delhi, for extending help in performing the MTT assay.

■ ABBREVIATIONS

DTNB, 5,5′-dithiol-bis(2-nitrobenzoic acid); ADMET, absorption, distribution, metabolism, elimination, and toxicity; Ach, acetylcholinesterase; AChE, acetylcholinesterase; AD, Alzheimer's disease; Aβ, amyloid β; APP, amyloid precursor protein; BACE1, β-site APP cleaving enzyme 1; DSSP, database of secondary structure assignments; DPBS, Dulbecco's phosphate-buffered saline; Eq, equation; FBS, fetal bovine serum; HPLC, high-performance liquid chromatography; HCl, hydrochloric acid; IC_{50}, inhibitory concentration; V_{max}, maximum reaction velocity; MTT, 3-(4,5-dimethylthiazol-2-yl)-2,5-diphenyltetrazolium bromide; MD, molecular dynamics; MM-PBSA, molecular mechanics Poisson−Boltzmann surface area; M_W, molecular weight; MTDL, multitarget-directed ligand; NCCS, National Centre for Cell Science; (nOH), number of hydrogen bond acceptors; OHNH, number of hydrogen bond donors; log P value, partition coefficient; PDB, protein data bank; R_g, radius of gyration; RMSD, root-mean square deviation; RMSF, root-mean square fluctuation; SDF, structure data file; SSC, secondary structure content; SASA, solvent-accessible surface area; K_m, substrate concentration at half V_{max}; 3D, three dimensional; 2D, two-dimensional

■ REFERENCES

(1) Nichols, E.; Szoeke, C. E. I.; Vollset, S. E.; Abbasi, N.; Abd-Allah, F.; Abdela, J.; Aichour, M. T. E.; Akinyemi, R. O.; Alahdab, F.; Asgedom, S. W.; Awasthi, A.; Barker-Collo, S. L.; Baune, B. T.; Béjot, Y.; Belachew, A. B.; Bennett, D. A.; Biadgo, B.; Bijani, A.; Bin Sayeed, M. S.; Brayne, C.; Carpenter, D. O.; Carvalho, F.; Catalá-López, F.; Cerin, E.; Choi, J.-Y. J.; Dang, A. K.; Degefa, M. G.; Djalalinia, S.; Dubey, M.; Duken, E. E.; Edvardsson, D.; Endres, M.; Eskandarieh, S.; Faro, A.; Farzadfar, F.; Fereshtehnejad, S.-M.; Fernandes, E.; Filip, I.; Fischer, F.; Gebre, A. K.; Geremew, D.; Ghasemi-Kasman, M.; Gnedovskaya, E. V.; Gupta, R.; Hachinski, V.; Hagos, T. B.; Hamidi, S.; Hankey, G. J.; Haro, J. M.; Hay, S. I.; Irvani, S. S. N.; Jha, R. P.; Jonas, J. B.; Kalani, R.; Karch, A.; Kasaeian, A.; Khader, Y. S.; Khalil, I. A.; Khan, E. A.; Khanna, T.; Khoja, T. A. M.; Khubchandani, J.; Kisa, A.; Kissimova-Skarbek, K.; Kivimäki, M.; Koyanagi, A.; Krohn, K. J.; Logroscino, G.; Lorkowski, S.; Majdan, M.; Malekzadeh, R.; März,

W.; Massano, J.; Mengistu, G.; Meretoja, A.; Mohammadi, M.; Mohammadi-Khanaposhtani, M.; Mokdad, A. H.; Mondello, S.; Moradi, G.; Nagel, G.; Naghavi, M.; Naik, G.; Nguyen, L. H.; Nguyen, T. H.; Nirayo, Y. L.; Nixon, M. R.; Ofori-Asenso, R.; Ogbo, F. A.; Olagunju, A. T.; Owolabi, M. O.; Panda-Jonas, S.; Passos, V. M.; de, A.; Pereira, D. M.; Pinilla-Monsalve, G. D.; Piradov, M. A.; Pond, C. D.; Poustchi, H.; Qorbani, M.; Radfar, A.; Reiner, R. C.; Robinson, S. R.; Roshandel, G.; Rostami, A.; Russ, T. C.; Sachdev, P. S.; Safari, H.; Safiri, S.; Sahathevan, R.; Salimi, Y.; Satpathy, M.; Sawhney, M.; Saylan, M.; Sepanlou, S. G.; Shafieesabet, A.; Shaikh, M. A.; Sahraian, M. A.; Shigematsu, M.; Shiri, R.; Shiue, I.; Silva, J. P.; Smith, M.; Sobhani, S.; Stein, D. J.; Tabarés-Seisdedos, R.; Tovani-Palone, M. R.; Tran, B. X.; Tran, T. T.; Tsegay, A. T.; Ullah, I.; Venketasubramanian, N.; Vlassov, V.; Wang, Y.-P.; Weiss, J.; Westerman, R.; Wijeratne, T.; Wyper, G. M. A.; Yano, Y.; Yimer, E. M.; Yonemoto, N.; Yousefifard, M.; Zaidi, Z.; Zare, Z.; Vos, T.; Feigin, V. L.; Murray, C. J. L. Global, Regional, and National Burden of Alzheimer's Disease and Other Dementias, 1990−2016: A Systematic Analysis for the Global Burden of Disease Study 2016. *Lancet Neurol.* **2019**, *18* (1), 88−106.

(2) Downer, B.; Al Snih, S.; Raji, M.; Chou, L.-N.; Kuo, Y.-F.; Markides, K. S.; Ottenbacher, K. J. Healthcare Utilization of Mexican-American Medicare Beneficiaries with and without Alzheimer's Disease and Related Dementias. *PLoS One* **2020**, *15* (1), No. e0227681.

(3) Srivastava, S.; Ahmad, R.; Khare, S. K. Alzheimer's Disease and Its Treatment by Different Approaches: A Review. *Eur. J. Med. Chem.* **2021**, *216*, No. 113320.

(4) Hafez, D. E.; Dubiel, M.; La Spada, G.; Catto, M.; Reiner-Link, D.; Syu, Y.-T.; Abdel-Halim, M.; Hwang, T.-L.; Stark, H.; Abadi, A. H. Novel Benzothiazole Derivatives as Multitargeted-Directed Ligands for the Treatment of Alzheimer's Disease. *J. Enzyme Inhib. Med. Chem.* **2023**, *38* (1), No. 2175821.

(5) Obaid, R. J.; Naeem, N.; Mughal, E. U.; Al-Rooqi, M. M.; Sadiq, A.; Jassas, R. S.; Moussa, Z.; Ahmed, S. A. Inhibitory Potential of Nitrogen, Oxygen and Sulfur Containing Heterocyclic Scaffolds against Acetylcholinesterase and Butyrylcholinesterase. *RSC Adv.* **2022**, *12* (31), 19764−19855.

(6) Xiao, Y.; Liang, W.; Liu, D.; Zhang, Z.; Chang, J.; Zhu, D. Isolation and Acetylcholinesterase Inhibitory Activity of Asterric Acid Derivatives Produced by Talaromyces Aurantiacus FL15, an Endophytic Fungus from Huperzia Serrata. *3 Biotech* **2022**, *12* (3), No. 60, DOI: 10.1007/s13205-022-03125-2.

(7) Budryn, G.; Majak, I.; Grzelczyk, J.; Szwajgier, D.; Rodríguez-Martínez, A.; Pérez-Sánchez, H. Hydroxybenzoic Acids as Acetylcholinesterase Inhibitors: Calorimetric and Docking Simulation Studies. *Nutrients* **2022**, *14* (12), No. 2476, DOI: 10.3390/nu14122476.

(8) Shi, Y.; Evans, R. M.; Gage, F. H. Oleic Acid Regulates Hippocampal Neurogenesis as a TLX Ligand. *Proc. Natl. Acad. Sci. U.S.A.* **2022**, *119* (15), No. e2203038119.

(9) Roda, A.; Serra-Mir, G.; Montoliu-Gaya, L.; Tiessler, L.; Villegas, S. Amyloid-Beta Peptide and Tau Protein Crosstalk in Alzheimer's Disease. *Neural Regener. Res.* **2022**, *17* (8), No. 1666, DOI: 10.4103/1673-5374.332127.

(10) Rajkumar, M.; Vimala, K.; Tamiliniyan, D. D.; Thangaraj, R.; Jaganathan, R.; Kumaradhas, P.; Kannan, S. Gelatin/Polyvinyl Alcohol Loaded Magnesium Hydroxide Nanocomposite Attenuates Neurotoxicity and Oxidative Stress in Alzheimer's Disease Induced Rats. *Int. J. Biol. Macromol.* **2022**, *222*, 2122−2143.

(11) Zhang, Q.; Sidorenko, J.; Couvy-Duchesne, B.; Marioni, R. E.; Wright, M. J.; Goate, A. M.; Marcora, E.; Huang, K.; Porter, T.; Laws, S. M.; Masters, C. L.; Bush, A. I.; Fowler, C.; Darby, D.; Pertile, K.; Restrepo, C.; Roberts, B.; Robertson, J.; Rumble, R.; Ryan, T.; Collins, S.; Thai, C.; Trounson, B.; Lennon, K.; Li, Q.-X.; Ugarte, F. Y.; Volitakis, I.; Vovos, M.; Williams, R.; Baker, J.; Russell, A.; Peretti, M.; Milicic, L.; Lim, L.; Rodrigues, M.; Taddei, K.; Taddei, T.; Hone, E.; Lim, F.; Fernandez, S.; Rainey-Smith, S.; Pedrini, S.; Martins, R.; Doecke, J.; Bourgeat, P.; Fripp, J.; Gibson, S.; Leroux, H.; Hanson, D.; Dore, V.; Zhang, P.; Burnham, S.; Rowe, C. C.; Villemagne, V. L.; Yates, P.; Pejoska, S. B.; Jones, G.; Ames, D.; Cyarto, E.; Lautenschlager, N.; Barnham, K.; Cheng, L.; Hill, A.; Killeen, N.; Maruff, P.; Silbert, B.; Brown, B.; Sohrabi, H.; Savage, G.; Vacher, M.; Sachdev, P. S.; Mather, K. A.; Armstrong, N. J.; Thalamuthu, A.; Brodaty, H.; Yengo, L.; Yang, J.; Wray, N. R.; McRae, A. F.; Visscher, P. M.; Australian Imaging Biomarkers and Lifestyle (AIBL) Study. Risk Prediction of Late-Onset Alzheimer's Disease Implies an Oligogenic Architecture. *Nat. Commun.* **2020**, *11* (1), No. 4799, DOI: 10.1038/s41467-020-18534-1.

(12) Hossain, T.; Mukherjee, A.; Saha, A. Chemometric Design to Explore Pharmacophore Features of BACE Inhibitors for Controlling Alzheimer's Disease. *Mol. BioSyst.* **2015**, *11* (2), 549−557.

(13) Pont, C.; Ginex, T.; Griñán-Ferré, C.; Scheiner, M.; Mattellone, A.; Martínez, N.; Arce, E. M.; Soriano-Fernández, Y.; Naldi, M.; De Simone, A.; Barenys, M.; Gómez-Catalán, J.; Pérez, B.; Sabate, R.; Andrisano, V.; Loza, M. I.; Brea, J.; Bartolini, M.; Bolognesi, M. L.; Decker, M.; Pallàs, M.; Luque, F. J.; Muñoz-Torrero, D. From Virtual Screening Hits Targeting a Cryptic Pocket in BACE-1 to a Nontoxic Brain Permeable Multitarget Anti-Alzheimer Lead with Disease-Modifying and Cognition-Enhancing Effects. *Eur. J. Med. Chem.* **2021**, *225*, No. 113779.

(14) Ahmad, R.; Srivastava, S.; Ghosh, S.; Khare, S. K. Phytochemical Delivery through Nanocarriers: A Review. *Colloids Surf., B* **2021**, *197*, No. 111389.

(15) Rehman, M.; AlAjmi, M.; Hussain, A.; Rather, G.; Khan, M. High-Throughput Virtual Screening, Molecular Dynamics Simulation, and Enzyme Kinetics Identified ZINC84525623 as a Potential Inhibitor of NDM-1. *Int. J. Mol. Sci.* **2019**, *20* (4), No. 819, DOI: 10.3390/ijms20040819.

(16) Rafi, M. O.; Bhattacharje, G.; Al-Khafaji, K.; Taskin-Tok, T.; Alfasane, Md. A.; Das, A. K.; Parvez, M. A. K.; Rahman, M. S. Combination of QSAR, Molecular Docking, Molecular Dynamic Simulation and MM-PBSA: Analogues of Lopinavir and Favipiravir as Potential Drug Candidates against COVID-19. *J. Biomol. Struct. Dyn.* **2022**, *40* (8), 3711−3730.

(17) Zhao, X.; Gong, D.; Jiang, Y.; Guo, D.; Zhu, Y.; Deng, Y. Multipotent AChE and BACE-1 Inhibitors for the Treatment of Alzheimer's Disease: Design, Synthesis and Bio-Analysis of 7-Amino-1,4-Dihydro-2 H -Isoquilin-3-One Derivates. *Eur. J. Med. Chem.* **2017**, *138*, 738−747.

(18) Ezz Eldin, R. R.; Saleh, M. A.; Alotaibi, M. H.; Alsuair, R. K.; Alzahrani, Y. A.; Alshehri, F. A.; Mohamed, A. F.; Hafez, S. M.; Althoqapy, A. A.; Khirala, S. K.; Amin, M. M.; A, F. Y.; AbdElwahab, A. H.; Alesawy, M. S.; Elmaaty, A. A.; Al-Karmalawy, A. A. Ligand-Based Design and Synthesis of *N′* -Benzylidene-3,4-Dimethoxybenzohydrazide Derivatives as Potential Antimicrobial Agents; Evaluation by *in Vitro*, *in Vivo, and in Silico* Approaches with SAR Studies. *J. Enzyme Inhib. Med. Chem.* **2022**, *37* (1), 1098−1119, DOI: 10.1080/14756366.2022.2063282.

(19) Choudhary, M. I.; Yousuf, S.; Nawaz, S. A.; Ahmed, S.; Atta-ur-Rahman. Cholinesterase Inhibiting Withanolides from Withania Somnifera. *Chem. Pharm. Bull.* **2004**, *52* (11), 1358−1361, DOI: 10.1248/cpb.52.1358.

(20) Choudhary, M. I.; Nawaz, S. A.; Zaheer-ul-Haq; Lodhi, M. A.; Ghayur, M. N.; Jalil, S.; Riaz, N.; Yousuf, S.; Malik, A.; Gilani, A. H.; Atta-ur-Rahman. Withanolides, a New Class of Natural Cholinesterase Inhibitors with Calcium Antagonistic Properties. *Biochem. Biophys. Res. Commun.* **2005**, *334* (1), 276−287.

(21) Grover, A.; Shandilya, A.; Agrawal, V.; Bisaria, V. S.; Sundar, D. Computational Evidence to Inhibition of Human Acetyl Cholinesterase by Withanolide A for Alzheimer Treatment. *J. Biomol. Struct. Dyn.* **2012**, *29* (4), 651−662.

(22) Hannan, M. A.; Dash, R.; Haque, M. N.; Choi, S. M.; Moon, I. S. Integrated System Pharmacology and In Silico Analysis Elucidating Neuropharmacological Actions of *Withania Somnifera* in the Treatment of Alzheimer's Disease. *CNS Neurol. Disord.: Drug Targets* **2020**, *19* (7), 541−556.

(23) Malik, M. Y.; Taneja, I.; Raju, K. S. R.; Gayen, J. R.; Singh, S. P.; Sangwand, N. S.; Wahajuddin, M. RP-HPLC Separation of Isomeric Withanolides: Method Development, Validation and

Application to In Situ Rat Permeability Determination. *J. Chromatogr. Sci.* **2017**, *55* (7), 729−735, DOI: 10.1093/chromsci/bmx027.
(24) Dev, S. *Prime Ayurvedic Plant Drugs: A Modern Scientific Appraisal*; Ane Books India, 2011.
(25) Watt, G. *The Wealth of India: Raw Material Series; National Institute of Science Communication and Information Resource*, CSIR, 1942.
(26) Kim, S.; Chen, J.; Cheng, T.; Gindulyte, A.; He, J.; He, S.; Li, Q.; Shoemaker, B. A.; Thiessen, P. A.; Yu, B.; Zaslavsky, L.; Zhang, J.; Bolton, E. E. PubChem 2019 Update: Improved Access to Chemical Data. *Nucleic Acids Res.* **2019**, *47* (D1), D1102−D1109.
(27) Cheung, J.; Gary, E. N.; Shiomi, K.; Rosenberry, T. L. Structures of Human Acetylcholinesterase Bound to Dihydrotanshinone I and Territrem B Show Peripheral Site Flexibility. *ACS Med. Chem. Lett.* **2013**, *4* (11), 1091−1096.
(28) Cumming, J. N.; Le, T. X.; Babu, S.; Carroll, C.; Chen, X.; Favreau, L.; Gaspari, P.; Guo, T.; Hobbs, D. W.; Huang, Y.; Iserloh, U.; Kennedy, M. E.; Kuvelkar, R.; Li, G.; Lowrie, J.; McHugh, N. A.; Ozgur, L.; Pan, J.; Parker, E. M.; Saionz, K.; Stamford, A. W.; Strickland, C.; Tadesse, D.; Voigt, J.; Wang, L.; Wu, Y.; Zhang, L.; Zhang, Q. Rational Design of Novel, Potent Piperazinone and Imidazolidinone BACE1 Inhibitors. *Bioorg. Med. Chem. Lett.* **2008**, *18* (11), 3236−3241.
(29) DeLano, W. L. *PyMOL*, 2020. pymol.org.
(30) Morris, G. M.; Goodsell, D. S.; Pique, M. E.; Lindstrom, W. *AutoDock4*, 2014.
(31) Gupta, A.; Sharma, P.; Jayaram, B. ParDOCK: An All Atom Energy Based Monte Carlo Docking Protocol for Protein-Ligand Complexes. *PPL* **2007**, *14* (7), 632−646.
(32) Systemes, D. BIOVIA Discovery Studio 2017. https://discover.3ds.com/discovery-studio-visualizer-download.
(33) Iqbal, D.; Khan, M. S.; Waiz, M.; Rehman, M. T.; Alaidarous, M.; Jamal, A.; Alothaim, A. S.; AlAjmi, M. F.; Alshehri, B. M.; Banawas, S.; Alsaweed, M.; Madkhali, Y.; Algarni, A.; Alsagaby, S. A.; Alturaiki, W. Exploring the Binding Pattern of Geraniol with Acetylcholinesterase through In Silico Docking, Molecular Dynamics Simulation, and In Vitro Enzyme Inhibition Kinetics Studies. *Cells* **2021**, *10* (12), No. 3533, DOI: 10.3390/cells10123533.
(34) Prasanth, D. S. N. B. K.; Singh, G.; Panda, S. P.; Achanti, S.; Soni, H.; Chaudhuri, T. K.; Pawar, H. A.; Jahasultana, M. In Silico Screening of Plant-Derived Anti-Virals from Shorea Hemsleyana (King) King Ex Foxw Against SARS CoV-2 Main Protease. *Chem. Afr.* **2023**, *6*, 345−366, DOI: 10.1007/s42250-022-00521-2.
(35) Mishra, D.; Fatima, A.; Kumar, P.; Munjal, N. S.; Singh, B. K.; Singh, R. Synthesis of Benzothiazole Linked Triazole Conjugates and Their Evaluation Against Cholinesterase Enzymes. *ChemistrySelect* **2022**, *7* (46), No. e202203060, DOI: 10.1002/slct.202203060.
(36) Van Der Spoel, D.; Lindahl, E.; Hess, B.; Groenhof, G.; Mark, A. E.; Berendsen, H. J. C. GROMACS: Fast, Flexible, and Free. *J. Comput. Chem.* **2005**, *26* (16), 1701−1718.
(37) Malde, A. K.; Zuo, L.; Breeze, M.; Stroet, M.; Poger, D.; Nair, P. C.; Oostenbrink, C.; Mark, A. E. An Automated Force Field Topology Builder (ATB) and Repository: Version 1.0. *J. Chem. Theory Comput.* **2011**, *7* (12), 4026−4037.
(38) Lemkul, J. From Proteins to Perturbed Hamiltonians: A Suite of Tutorials for the GROMACS-2018 Molecular Simulation Package [Article v1.0] *LiveCoMS* 2019; Vol. *1* 1 DOI: 10.33011/livecoms.1.1.5068.
(39) Bhatia, N. K.; Modi, P.; Sharma, S.; Deep, S. Quercetin and Baicalein Act as Potent Antiamyloidogenic and Fibril Destabilizing Agents for SOD1 Fibrils. *ACS Chem. Neurosci.* **2020**, *11* (8), 1129−1138.
(40) Sharma, S.; Deep, S. In-Silico Drug Repurposing for Targeting SARS-CoV-2 Main Protease (M^{pro}). *J. Biomol. Struct. Dyn.* **2022**, *40* (7), 3003−3010.
(41) Kumari, R.; Kumar, R.; Lynn, A.; Open Source Drug Discovery Consortium. *G_mmpbsa* —A GROMACS Tool for High-Throughput MM-PBSA Calculations. *J. Chem. Inf. Model.* **2014**, *54* (7), 1951−1962, DOI: 10.1021/ci500020m.
(42) Loschwitz, J.; Jäckering, A.; Keutmann, M.; Olagunju, M.; Eberle, R. J.; Coronado, M. A.; Olubiyi, O. O.; Strodel, B. Novel Inhibitors of the Main Protease Enzyme of SARS-CoV-2 Identified via Molecular Dynamics Simulation-Guided in Vitro Assay. *Bioorg. Chem.* **2021**, *111*, No. 104862.
(43) Alara, O. R.; Abdurahman, N. H.; Ukaegbu, C. I. Extraction of Phenolic Compounds: A Review. *Curr. Res. Food Sci.* **2021**, *4*, 200−214.
(44) Zhang, Q.-W.; Lin, L.-G.; Ye, W.-C. Techniques for Extraction and Isolation of Natural Products: A Comprehensive Review. *Chin. Med.* **2018**, *13* (1), No. 20, DOI: 10.1186/s13020-018-0177-x.
(45) Ha, J. W.; Yu, J. S.; Lee, B. S.; Kang, D.-M.; Ahn, M.-J.; Kim, J. K.; Kim, K. H. Structural Characterization of Withanolide Glycosides from the Roots of Withania Somnifera and Their Potential Biological Activities. *Plants* **2022**, *11* (6), No. 767, DOI: 10.3390/plants11060767.
(46) Guo, Y.; Yang, H.; Huang, Z.; Tian, S.; Li, Q.; Du, C.; Chen, T.; Liu, Y.; Sun, H.; Liu, Z. Design, Synthesis, and Evaluation of Acetylcholinesterase and Butyrylcholinesterase Dual-Target Inhibitors against Alzheimer's Diseases. *Molecules* **2020**, *25* (3), No. 489, DOI: 10.3390/molecules25030489.
(47) Nuria, M. C.; Suganda, A. G.; Sukandar, E. Y.; Insanu, M. Acetylcholinesterase: Inhibitory Activity of Some Indonesian Vegetables and Fraction of Selected Plants. *J. Appl. Pharm. Sci.* **2020**, *10* (1), 101−107, DOI: 10.7324/JAPS.2020.101014.
(48) Mphahlele, M. J.; Agbo, E. N.; More, G. K.; Gildenhuys, S. In Vitro Enzymatic and Kinetic Studies, and In Silico Drug-Receptor Interactions, and Drug-Like Profiling of the 5-Styrylbenzamide Derivatives as Potential Cholinesterase and β-Secretase Inhibitors with Antioxidant Properties. *Antioxidants* **2021**, *10* (5), No. 647, DOI: 10.3390/antiox10050647.
(49) Agbo, E. N.; Gildenhuys, S.; Choong, Y. S.; Mphahlele, M. J.; More, G. K. Synthesis of Furocoumarin−Stilbene Hybrids as Potential Multifunctional Drugs against Multiple Biochemical Targets Associated with Alzheimer's Disease. *Bioorg. Chem.* **2020**, *101*, No. 103997, DOI: 10.1016/j.bioorg.2020.103997.
(50) Goel, S.; Mishra, P. Thymoquinone Loaded Mesoporous Silica Nanoparticles Retard Cell Invasion and Enhance in Vitro Cytotoxicity Due to ROS Mediated Apoptosis in HeLa and MCF-7 Cell Lines. *Mater. Sci. Eng.: C* **2019**, *104*, No. 109881.
(51) Jaiswal, S.; Mishra, P. Co-Delivery of Curcumin and Serratiopeptidase in HeLa and MCF-7 Cells through Nanoparticles Show Improved Anti-Cancer Activity. *Mater. Sci. Eng.: C* **2018**, *92*, 673−684.

https://doi.org/10.1021/acsomega.3c04261
ACS Omega 2023, 8, 38118−38129